Myosin 1f-mediated Activation of Microglia Contributes to the Photoreceptor Degeneration in a Mouse Model of Retinal Detachment

Yimin Wang
Shanghai First People's Hospital: Shanghai Jiaotong University First People's Hospital
Xiaohuan Zhao
Shanghai First People's Hospital: Shanghai Jiaotong University First People's Hospital
Min Gao
Shanghai First People's Hospital: Shanghai Jiaotong University First People's Hospital
Xiaoling Wan
Shanghai First People's Hospital: Shanghai Jiaotong University First People's Hospital
Yinong Guo
Shanghai First People's Hospital: Shanghai Jiaotong University First People's Hospital
Yingying Qu
Shanghai First People's Hospital: Shanghai Jiaotong University First People's Hospital
Yuhong Chen
Shanghai First People's Hospital: Shanghai Jiaotong University First People's Hospital
Tong Li
Shanghai First People's Hospital: Shanghai Jiaotong University First People's Hospital
Haiyun Liu
Shanghai First People's Hospital: Shanghai Jiaotong University First People's Hospital
Mei Jiang
Shanghai First People's Hospital: Shanghai Jiaotong University First People's Hospital
Feng Wang
Shanghai First People's Hospital: Shanghai Jiaotong University First People's Hospital
Xiaodong Sun (xdsun@sjtu.edu.cn)
Shanghai Key Laboratory of Ocular Fundus Diseases, Shanghai General Hospital, Shanghai Engineering Center of Visual Science and Photomedicine, Shanghai 200080, China https://orcid.org/0000-0001-5015-0945

Research

Keywords: retinal detachment, photoreceptor degeneration, cell death, microglia, myosin 1f

Posted Date: October 1st, 2020

DOI: https://doi.org/10.21203/rs.3.rs-80015/v1

Version of Record: A version of this preprint was published at Cell Death & Disease on October 1st, 2021.
See the published version at https://doi.org/10.1038/s41419-021-03983-3.

Myosin 1f-mediated Activation of Microglia Contributes to the Photoreceptor Degeneration in a Mouse Model of Retinal Detachment

Yimin Wang,[1,2,3,4,*] Xiaohuan Zhao,[1,2,3,4,*] Min Gao,[1] Xiaoling Wan,[1,2,3] Yinong Guo,[1,2,3] Yingying Qu,[1,5] Yuhong Chen,[1,2,3] Tong Li, [1,2] Haiyun Liu,[1,2] Mei Jiang,[1,2,3] Feng Wang,[5,#] Xiaodong Sun[1,2,3,4,#]

1. Shanghai General Hospital , Shanghai Jiao Tong University School of Medicine
2. National Clinical Research Center for Eye Disease
3. Shanghai Key Laboratory of Ocular Fundus Diseases
4. Shanghai Engineering Center for Visual Science and Photomedicine
5. Shanghai Institute of Immunology, Translational Medicine Center, Shanghai General Hospital, State Key Laboratory of Oncogenes and Related Genes, Shanghai Jiao Tong University School of Medicine

#Corresponding author:

Dr. Xiaodong Sun and Dr. Feng Wang should be considered equivalent corresponding authors.

Xiaodong Sun, xdsun@sjtu.edu.cn

Department of Ophthalmology, Shanghai General Hospital, Shanghai Jiao Tong University School of Medicine, 100 Hai Ning Road, Shanghai 200080, P.R. China

Tel: +86-021-36126305; Fax: +86-021-63240825

Feng Wang, wangfeng16@sjtu.edu.cn

Shanghai Institute of Immunology, Translational Medicine Center, Shanghai General Hospital, State Key Laboratory of Oncogenes and Related Genes, Shanghai Jiao Tong University School of Medicine.
Tel: +86-021-53594658

* Yimin Wang and Xiaohuan Zhao contributed equally to this study and share the first authorship.

Financial Disclosures:
There are no financial conflicts of interest to disclose.

Funding: This study was supported by the National Natural Science Foundation of China （81730026，81771739）National Science and Technology Major Project (2017YFA0105301，2019ZX09301113，SQ2018YFA090045-01),Science and Technology Commission of Shanghai Municipality（17411953000，19495800700, 18JC1414100）, the Program for Professor of Special Appointments (Eastern Scholar) at Shanghai Institutions of Higher Learning, the Top Young Talent Program of Shanghai, and the Innovative Research Team of High-level Local Universities in Shanghai.

Abstract

Background: Photoreceptor death and neurodegeneration is the leading cause of irreversible vision loss. The inflammatory response of microglia plays an important role in the process of neurodegeneration. In this study, we examined the involvement of myosin 1f as a key regulator of immune cell activation via the AKT and MAPK pathways in microglia.

Methods: We chose retinal detachment as the model of photoreceptor degeneration. Immunofluorescence and Western Blot was performed to confirm the expression and location of myosin 1f in detached retina. The RD mouse model was induced in WT and myosin 1f-/- mice and confirmed by HE and TUNEL staining. The expression of inflammatory cytokine and downstream pathways was assessed via qPCR and WB.

Results: Myosin 1f was upregulated after retinal detachment, and it was specifically expressed in microglia. Deficiency of myosin 1f protected against cell death by inhibiting microglia activation. The elimination of microglia can abolish the protective effect of myosin 1f deficiency. After stimulation by LPS,

microglia with myosin 1f deficiency showed downregulation of the MAPK and AKT pathways.

Conclusions: Myosin 1f plays a crucial role in microglia-induced neuro-inflammation after retinal injury and photoreceptor degeneration by regulating 2 classic pathways, MAPK and AKT, and thereby decreasing the expression of inflammatory cytokines. Myosin 1f can be inhibited to prevent a decline in visual acuity after photoreceptor degeneration.

Key Words: retinal detachment, photoreceptor degeneration. cell death, microglia, myosin 1f

Background

The loss of photoreceptors and retinal function disorder is the feature of photoreceptor degeneration, which leads to the irreversible vision loss [1]. The pathogenesis is involved in many retinal diseases, including retinal detachment, retinitis pigmentosa and age-related macular degeneration. In particular, retinal detachment is a kind of disease that photoreceptors lose nutritional support after being separated from the retinal pigment epithelium (RPE) layer and choroidal vessels, which leads to the death of photoreceptors [2]. Rhegmatogenous retinal detachment (RRD) is the most common form of retinal detachment (RD), with an incidence of 13 per 100,000 persons annually [3]. Although surgery can reattach the retina with a high success rate, a small portion of patients still experience vision loss due to photoreceptor death [4, 5]. Therefore, discovering the mechanisms of the process of cell death is crucial to neuroprotection and intervention.

Although many death effectors have been discovered and targeted to prevent the loss of photoreceptors, little progress on rescuing photoreceptor

function after retinal injury [6]. Recently, transcriptome analysis has revealed that inflammatory responses play an important role in the process of photoreceptor degeneration [1, 7]. Many chemokines—such as TNF-α, IL-1β, IL-6, IL-8, and MCP-1—can reach a high level after 1 hour following retinal detachment [8, 9]. These cytokines can activate microglia and recruit macrophages in the sub-retinal space [1]. In the meantime, the activated microglia can release MCP-1, which contributes to the increased expression of MCP-1 in Müller cells and macrophages [10]. The positive feedback aggravates immune response and maintains a high level of neuro-inflammation [1, 11], which can be harmful to photoreceptors [2].

Microglia play a key role in the inflammatory feedback loop, which is a potential therapeutic target for neuroprotection in retinal degeneration. Activated microglia can express TNF-α and IL-1β, which are widely implicated in retinal degenerative disease. TNF-α can combine with TNF receptors 1 and 2, which are distributed on the membranes of neurons, leading to cytotoxicity by causing mitochondrial dysfunction and oxidative stress. IL-1β

104 is able to combine with interleukin receptors and leads to cell death in a
105 manner similar to TNF-α signaling [12, 13]. Meanwhile, it secretes MCP-1 to
106 recruit and activates astrocytes and immune cells from circulation, aggravating
107 the immune response [1, 11, 14]. Thus, it is important to discover the
108 mechanisms by which microglia affect this loop in order to potentially inhibit the
109 over-activation of microglia and the release of toxic cytokines. Mitogen-
110 activated protein kinases (MAPKs) regulates the expression of pro-
111 inflammatory cytokines such as TNF-α, IL-1β, and IL-6 [15]. Activated protein
112 kinase B (PKB), also named as AKT, can regulate inflammatory response by
113 downstream factors[16]. However, the upstream mechanism is not entirely
114 understood.

115 The myosin family, as a component of the cytoskeleton, has been reported
116 to play a crucial role in cell signaling [17, 18]. It is also a well-known component
117 of skeletal muscle in particular, in which it facilitates contractions [19]. In
118 addition, the delivery of intercellular material cannot occur without myosins;
119 they help the vesicles transport materials along the actin filament tracks [20].

Class 1 myosins have been revealed to be key components during pinocytosis [21], phagocytosis [22], cell motility [23], and secretion [24]. Therefore, the exploration of myosin function in microglia can lead to a better understanding of pathogenesis after retinal detachment. In this study, we have proven that myosin 1f is involved in the activation of microglia by regulating the MAPK and AKT pathways in mouse models of photoreceptor degeneration.

Methods

Sequencing data extraction and bioinformatics analysis

The sequencing data (GSE28133) were downloaded from GEO (https://www.ncbi.nlm.nih.gov/geo/query/acc.cgi?acc=GSE28133), which is a public database of chips and microarrays. The data contain 38 human retinal samples, including 19 samples from RD patients and 19 control samples without RD.

The data were normalized first, then DEGs were analyzed by a limma algorithm using the R programming language. The log fold change cutoff and

adjusted p value were set as 1 and 0.05, respectively. Points without gene symbols were removed.

A GO enrichment analysis of DRGs was obtained using the online tool DAVID (https://david.ncifcrf.gov /home.jsp, version 6.8). The bubble maps were drawn using Hmisc and ggplot2 via the R programming language. The GSEA analysis was conducted using GSEA_4.0.1 software.

Retinal detachment model animals

Myosin 1f-/- mice were purchased from Jackson Laboratory, then bred in the Shanghai General Hospital animal facility. All animal experiment protocols were in agreement with the Statement of the Association for Research in Vision and Ophthalmology for biomedical research. The animals were randomly assigned into 2 groups.

We used 1% atropine sulphate oculentum (Santen, Japan) and 0.5% tropicamide (Santen, Japan) on the ocular surface of mice to dilate the pupil. We applied 0.4% oxybuprocaine eye drops (Santen, Japan) as a surface

anesthesia. The mice were anesthetized using isoflurane gas (1.5% mixed with 50% air and 50% O^2). We applied 0.3% ofloxacin oculentum (Shanghai, China) as a magnifying lens to obtain a clearer view.

The examination of the RD model was conducted as previously described [25, 26]. The sclera was exposed and punctured at 2 mm posterior to the limbus with a 34-gauge needle. The vitreous humor was slowly aspirated with a 34G glass needle until the retina separated spontaneously from the underlying RPE layer. Then the 34G needle tip was inserted into the subretinal space through the same scleral hole, and sodium hyaluronate (HA, Shanghai, China) was gently injected. The fundus was observed and injection was halted after the retina was detached in every quadrant. The scleral hole was then sealed using cyanoacrylate surgical glue to prevent HA leakage. Finally, tobramycin and dexamethasone ointments (Alcon, USA) were applied to the ocular surface to prevent infection.

Immunofluorescence

The eyeballs were fixed in 4% paraformaldehyde and cut to a thickness of 10 μm to fabricate eye sections. We removed the chamber and kept the entire retina to prepare for the retinal stretched preparation after fixation.

We stained for the following antibodies: IBA-1 (1:1,000, Wako, 019–19741), F4/80 (1: 1,000, Abcam, 6640), GFAP (1: 1,000, Abcam, 4674), and myosin 1f (1: 1,000, Abcam, ab197215). The immunofluorescence was observed under a confocal microscope (Leica TCS SP8 confocal 137 microscope, Germany) and quantitatively analyzed using ImageJ software (Fiji, NIH, USA).

HE stains and ONL thickness

After being fixed in 4% paraformaldehyde, the eyeballs were embedded in paraffin and sectioned into 10-μm slices. The eye sections were stained with hematoxylin and eosin. We measured 10 points of thickness within the outer nuclear layer (ONL) on 1 section with the same spacing distance. The measurements were taken using ImageJ software (Fiji, NIH, USA).

184 *TUNEL assay*

185 In-Situ Cell Death Detection Kits (Roche, Germany) were applied to the eye
186 sections to detect apoptosis. The sections were permeated with 0.1% Triton X-
187 100 in 1% sodium citrate for 10 minutes, then they were incubated with a
188 TUNEL reaction mixture for 1 hour at 37 °C. The sections were observed under
189 the confocal microscope, and all TUNEL-positive cells were counted.

190

191 *Cell culture and myosin 1f knockdown*

192 We grew the immortalized murine microglial BV2 cell line at the same time
193 because BV2 can be a good substitute for primary microglia in many
194 experimental settings [27]. Small interfering RNA (siRNA) of myosin 1f (768:
195 CCACAUCUACUACCAGCUUTT AAGCUGGUAGUAGAUGUGGTT; 1413:
196 GCAGGAGGAGUAUGUGCAATT UUGCACAUACUCCUCCUGCTT; 2662:
197 GCGGACAGCUUCUUAGAAATT UUUCUAAGAAGCUGUCCGCTT) and
198 TransIT-2X (MIR 6000, Mirus) were chosen for the knockdown of myosin 1f.

For stimulation, 100 ng/ml of lipopolysaccharide (LPS, L2880, Sigma Aldrich, St. Louis, USA) was applied after 24 hours.

Western blot analysis

Retina and cell samples were lysed in a lysis buffer containing 50 mM Tris-HCl (pH 8.0) and 0.1% SDS, as well as the complete Protease Inhibitor Cocktail (11697498001; Roche Applied Science), 150 mM NaCl, 1% Triton X-100, and 1% sodium deoxycholate. We incubated the primary antibodies overnight. The antibodies were as follows: GAPDH (Proteintech, 60004-1-Ig, RRID: AB_2107436; Proteintech, Chicago, IL, USA), AKT (C67E7, Rabbit mAb, CST), p-AKT (Ser473, D9E, XP, Rabbit mAb, CST), ERK1/2 (137F5, Rabbit mAb, CST), p-ERK1/2 (D13.14.4E, XP, Rabbit mAb), JNK (#9252, CST), p-JNK (81E11, Rabbit mAb #4668, CST).

ELISA procedures

TNF-α and IL-1β were detected by using ELISA kits according to the manufacturer's protocols (MTA00B, MLB00C, R&D Systems, Minneapolis, USA). The tissue samples were lysed in PBS, and the supernatant was collected. The cell samples were then collected from the cultural supernatant.

Quantitative real-time PCR

The primer sequences were acquired from Primerbank (bankhttps://pga.mgh.harvard.edu/primerbank/), including TNF- α (F: CCCTCACACTCAGATCATCTTCT, R: GCTACGACGTGGGCTACAG), IL-1β (F: GAAATGCCACCTTTTGACAGTG, R: TGGATGCTCTCATCAGGACAG), IL-6 (F: TAGTCCTTCCTACCCCAATTTCC, R: TTGGTCCTTAGCCACTCCTTC), and myosin 1f (F: CTTTCACTGGCAGAGTCACAA, R: ATGAAGCGTTTGCGGAGGTT).

Photography and optical coherence tomography (OCT) in vivo

The mice were anesthetized before the operation. Fundus photography and optical coherence tomography were performed on eyes with dilated pupils. The equipments were purchased from Phoenix Research Labs, Inc. systems (Phoenix, USA).

Data and statistical analysis

The statistical analysis was conducted using Prism8 software. The data are presented as mean±SEM, unpaired t-test, $*p < 0.05$, $**p < 0.01$, $***p < 0.001$, $****p < 0.0001$; $p > 0.05$ was regarded as insignificant.

Results

Myosin 1f is upregulated after retinal detachment

We analyzed the data of GSE28133 from GEO datasets, which included 19 retinal tissues from retinal detachment patients and 19 control samples without ocular disease. A differential expression analysis revealed that 990 genes were upregulated and 272 genes were downregulated (|FC| >1.5 and $p<0.05$) (Figure

1A). As we expected, GO analysis indicated that immune response was involved in the pathology of RD (Figure 1B, 1C). GSEA enrichment analysis also confirmed the results (Figure 1D) that immune response was positively correlated to the RD group (Supplementary 1, Figure A). To discover the expression pattern of myosins after RD, a heat map was examined and revealed that several myosins were upregulated, including MYO1F, MYO3A, and MYO5C, in the RD groups (Figure 1E), and MYO1F was the most upregulated among the 3, with an FC of 1.786 (Figure 1F). To figure out the expression pattern of MYO1F along with time, we divided the patients into 3 groups according to the RD duration, including within one month, 1 month to 3 months and more than 3 months. The fold change MYO1F is the highest among the patients with a RD duration within one month (FC=2.19493181) (Figure 1G), suggesting an upregulation of MYO1F in the early phase.

To verify the results of the RNA sequencing, we detected the expression of myosin 1f in mouse retina samples. A western blot revealed that myosin 1f was upregulated on the detached retina, and it reached the peak at day 3 after

detachment (Figure 2A). Retinal injury always occurs with inflammation because microglia can be activated after the injury. We examined the location of myosin 1f via immunofluorescence. Immunofluorescence confirmed that myosin 1f was upregulated within the retinal section after RD, and it was co-located with microglia markers, including F4/80 and IBA1 (Figure 2B, C). Thus, myosin 1f is specifically expressed in microglia; there was no sign of co-location between myosin 1f and GFAP (Figure 2D).

We also confirmed the expression of myosin 1f in the other 2 models of photoreceptor degeneration. *Rd1* mouse is a model for retinitis pigmentosa, which is also characterized by photoreceptor death and microglia activation [28]. Light damage is another model of photoreceptor degeneration [29, 30]. We discovered the same expression pattern of myosin 1f in both the *rd1* mouse model (Figure 2E) and the light damage model (Figure 2F). Similarly, myosin 1f was expressed on F4/80 positive cells within the retina sections of the *rd1* mouse model (Figure 2G) and the light-damaged eye (Figure 2H).

Myosin 1f deficiency protects against photoreceptor death

To further study the function of myosin 1f, we investigated its effect on photoreceptor death in a myosin 1f-/- mouse model [18, 31, 32]. To verify that myosin 1f deficiency does not contribute to retinal injury and photoreceptor death, we observed the structure and function of the retina. Twenty-week-old myosin 1f-/- mice were compared with age-matched wild types and showed normal structures on both optical coherence tomography (Supplementary 2, Figure A, B) and HE section (Supplementary 2, Figure C, D), and the amplitude of electroretinograms (ERGs) for both groups were within the normal range (Supplementary 2, Figure E).

We chose RD model as a representative model of photoreceptor degeneration, then observed the myosin 1f-/- mice at 3 days after RD (Figure 3A) because it is reported that the apoptosis of photoreceptors is the most extensive at the 3rd day. Fundus photography and HE staining showed that the retina remained detached at the 3rd day (Supplementary 3, Figure A, B). To assess photoreceptor loss, we calculated the thickness of the outer nuclear

293 layer (ONL) (Figure 3B). Myosin 1f-/- mice exhibited thicker ONLs after RD
294 (Figure 3C). In addition, there were fewer TUNEL-positive cells in the myosin
295 1f-/- (Figure 3D, 3E), which suggests that myosin 1f deficiency can protect
296 against photoreceptor apoptosis.
297
298 *Myosin 1f influences microglia activation*
299 We analyzed the morphology of microglia 3 days after RD via stretched
300 preparation and immunofluorescence. The microglia were more extended and
301 had more branches in the retina of myosin 1f-/- mice, whereas the microglia of
302 WT retina were more shrunken and tended to be round (Figure 4A). A
303 quantitative skeleton analysis and a Sholl analysis showed more intersections
304 in the myosin 1f-/- group (Figure 4B, 4C). This indicates that myosin 1f may
305 contribute to microglia activation. We have also counted the IBA1+ cells of the
306 stretched preparation and cell counts on the retina of myosin 1f-/- showed no
307 difference (Supplementary 3, Figure C). Microglia can migrate to injury site after

RD, especially outer nuclear layer (ONL), however, we have not observed the difference in numbers of infiltrated microglia (Supplementary 3, Figure D).

To evaluate the inflammation status of the retina and the function of microglia in the myosin 1f-/- group after RD, we detected the expression levels of inflammation markers and signature cytokines. IL-1β, IL-6 and TNF- α are classic pro-inflammatory cytokines in activated microglia [33]. The ELISA analysis suggests IL-1β (Figure 4D) and TNF- α (Figure 4E) was also downregulated in myosin 1f-/- mice at day 3. The mRNA expression is in accordance with the protein expression pattern. We observed the downregulation of IL-1β, TNF- α, and IL-6 in myosin 1f-/- mice at day 3, compared to WT mice (Figure 4F). In addition, CD68, a marker related to the degree of activation [34, 35], was lower at day 1 in myosin 1f-/- mice (Figure 4G).

Elimination of microglia can abolish the protective effect of myosin 1f deficiency

To verify that myosin 1f deficiency can protect photoreceptors by regulating the activation of microglia, we administered PLX3397 [36] to mice via oral gavage to eliminate mononuclear phagocytes, including microglia. PLX3397 is an inhibitor of the CSF1R receptor, which is widely expressed in mononuclear phagocytes [37]. It is reported that PLX3397 can reduce tissue macrophages without affecting myeloid cells [38]. We started gavage at day 1, and a dose was delivered every day until day 7. We conducted the RD model experiment at day 4 and observed at day 7 (Figure 5A).

The retinal thickness and the TUNEL-positive cells were calculated to evaluate photoreceptor death. There was no difference in ONL thickness between the 2 groups after PLX3397. Likewise, there were no significant differences in TUNEL-positive cell counts between the 2 groups (Figure 5B, 5C). We then detected mRNA expression after microglia elimination. Interestingly, the difference in CD68 between the 2 groups disappeared (Figure 5D). Similarly, the mRNA expression of IL-1β and TNF-α also disappeared

(Figure 5E). That is to say, microglia elimination abolished the protective effect of myosin 1f deficiency.

Myosin 1f affects microglia activation by regulating the MAPK/ AKT pathways

To further explore the molecular mechanism underlying myosin 1f – mediated photoreceptor degeneration, we used lipopolysaccharide (LPS), a pathogen-associated molecular pattern (PAMP) to stimulate BV2 cell lines in vitro. BV2 is an immortalized cell line derived from mice [39]. We noticed the upregulation of myosin 1f after stimulation (Figure 6A). The transcription level of IL-1β rose 6 hours after stimulation. In addition, an ELISA analysis suggests that TNF-α rose after LPS stimulation (Figure 6B). Furthermore, we developed a siRNA knockdown system for myosin 1f. We designed 3 sequences of siRNA, including 768, 1413, and 2662; all of them led to a significant decrease of myosin 1f at the protein level (Figure 6C). We chose 2662 to detect the quantitative efficiency of the siRNA, and the efficiency reached about 80% (Figure 6D).

We used LPS to stimulate the control and myosin 1f knockdown cells. Then we detected the expression of IL-1β and TNF-α in the cellular supernatant at hour 24 via ELISA, and we found that both cytokines went down in the knockdown group (Figure 6E).

Previous studies showed that MAPK and AKT signaling pathways have been implicated in the activation of microglia. We then detected the expression of proteins related to MAPK and AKT. The proportion of phospho-AKT decreases after 24 hours of LPS stimulation (Figure 6F). As the 2 main components of MAPK, phospho-ERK and phospho-JNK also showed significant decreases. In addition, we repeated western blot to detect the phosphorylation protein in the detached retina of WT and myosin 1f mice (Figure 6G). In vivo results may further verify the consequences of myosin 1f regulation of microglia activity through the MAPK and AKT pathways.

Discussion

In the current study, we have discovered that myosin 1f was significantly upregulated after photoreceptor degeneration in both human retina and mouse model. We further demonstrated that myosin 1f can regulate microglia activation, whereas the absence of myosin 1f can protect photoreceptors by inhibiting the MAPK and AKT pathways and decreasing the expression of inflammatory cytokines, such as TNF-α and IL-1β, in microglia.

The vision loss after RD is mainly due to photoreceptor death [40]. Various forms of cell death are involved in this pathology, including apoptosis, necrosis, and autophagy, which peak at 2 to 3 days after RD [41]. Despite the discovery and inhibition of downstream effectors in cell death, no current techniques can stop photoreceptor death completely [6]. This indicates that cell death is a complicated process involving different pathologies, including inflammation. The sequence of the human retina sample after RD demonstrated that immune response and neurodegeneration are 2 major biological processes involved in RD [7].

Besides, we have discovered that myosin 1f was up-regulated after photoreceptor degeneration. Myosins, as a family of molecular motors, have various functions in the cell, including cell transformation, cell motility, material transportation within cells, and signal transduction [42]. Furthermore, myosin 1f, a class 1 myosin, can regulate the immune response [43, 44]. It is reported that myosin 1f is not only involved in the M1 polarization of macrophages by stimulating intercellular adhesion [45] but also influences neutrophil migration [32]. In our study, we found that myosin 1f was the most upregulated myosin by re-analyzing human RD sequence data, and we verified the results in a mouse RD model. We also found that myosin 1f is generally upregulated in *rd1* mutation mouse model and light-induced retinal injury. The *rd1* mutation mouse is a classical model for retinitis pigmentosa, with the rod photoreceptor degeneration at postnatal day 8[46]. Microglia are activated and express inflammatory cytokines in *rd1* mouse model retina. A similar pathology occurs in light-induced injury. Thus, we discovered that myosin 1f was also upregulated in the 2 latter cases, which suggests it could play a key role in

400 photoreceptor degeneration. It is reported that myosin 1f is also upregulated in
401 brain neurodegeneration, such as Alzheimer's disease (AD), Huntington's
402 disease (HD), and Parkinson's disease (PD) [47], suggesting the upregulation
403 of myosin 1f is a common phenomenon in neuro-inflammation.

404 We also discovered that myosin 1f is highly expressed in microglia. Via
405 immunofluorescence, we found that myosin 1f displayed a strong co-
406 localization with mononuclear macrophages but not Müller cells, indicating a
407 possible relationship between myosin 1f and microglia activation after retinal
408 injury. Though myosin 1f is involved in the motility of neutrophils[31], it is
409 surprising that myosin 1f does not affect the migration of microglia to injury site.
410 Instead, it affects the morphology of microglia, suggesting that the function of
411 myosin 1f could be various among different immune cell types.

412 To further determine the function of myosin 1f, we used a myosin 1f KO
413 mouse model to observe the difference. The KO mouse model showed a
414 significant reduction in neuron death. It suggested that myosin 1f deficiency

415 could be protective to neurons and it is possible to work by affecting the
416 activation of microglia.

417 Microglia, as a resident immune cell, is among the main effector cells of
418 neuroinflammation after retinal injury [48]. In our study, we have discovered that
419 myosin 1f deficiency have reduced the expression of inflammatory cytokines
420 such as TNF-α and IL-1β. Besides, we found the morphological difference of
421 microglia in myosin 1f KO retina and WT retina after RD. After the elimination
422 of microglia, the protective effect of myosin 1f KO disappeared. Therefore, we
423 think myosin 1f can regulate the activation of microglia and involved in neuro-
424 inflammation, which leads to the death of photoreceptors. In fact, the function
425 of microglia in physiological and pathological conditions remains unclear [49].
426 It is a double-edged sword; although over-activated microglia can release
427 cytotoxic factors that lead to neuron death [50, 51], it can also protect neurons
428 by secreting neuroprotective factors and phagocytosing injured cells [52]. The
429 state of microglia can be decided by the course of the disease, the immune
430 microenvironment, and interactions with other cells. Still and all, the two states

of microglia are dynamic and coexist. Discovering a way to inhibit the inflammation pathway is still a promising target for retinal degeneration.

We discovered that myosin 1f can regulate the MAPK and AKT pathway to promote the transcription of pro-inflammatory cytokines and activate microglia. Mitogen-activated protein kinases (MAPK) signal the transduction pathway, which consists of ERKs, c-Jun NH2-terminal kinases (JNKs), and p38 MAPKs and is reported to be related to inflammation, cell proliferation, and apoptosis [53, 54]. It is also associated with microglia-induced neuro-inflammation and the secretion of neurotoxic cytokines [55, 56]. AKT is an important protein of signaling transduction, which is involved in multiple pathways[16], and it can promote the expression of pro-inflammatory cytokines [57]. AKT can also be an upstream regulator of NF-κb pathway [58]. NF-κb is a classic, crucial transcription factor in both innate and adaptive immune responses, and it participates in microglia induced neuro-inflammation [59, 60]. Our results reveal that myosin 1f could be the common upstream of MAPK and AKT pathways, making it a promising target for neuroprotective approaches.

447 Myosins can influence signaling in several ways, through phosphorylation,
448 receptor recycling, interaction with integrin, and so on [61, 62]. Class II myosin
449 can increase the integrin β1 activity by clustering, and integrin β1 is required
450 for the activation of AKT pathway[62]. Myosin 1C, myosin 1E and myosin 1G
451 can regulate TGF- β signaling by regulating the recycling and redistribution of
452 TGF- β receptors to cell membrane. Myosin 1f may work in a similar way,
453 however, more future researches are needed to explore the interaction of
454 myosin 1f and downstream pathways.

455 In this study, we have revealed the the function of myosin 1f in neuro-
456 inflammation, through the regulation of microglia activation. We wondered that
457 the up-regulation of myosin 1f may be universal in other retinal degeneration
458 models, such as light damage and *rd1* mouse model, since microglia is usually
459 activated when encountering retinal injury. Our finding may provide a new
460 perspective for neuro-protection in photoreceptor degeneration. It is reported
461 that several compounds have been discovered as the inhibitors of myosins,
462 such as pentachloropseudilin (PCLP), a pseudilin derivative, which is a class

463 one myosin specific inhibitor [63, 64]; Blebbistatin [65], a myosin-2 inhibitor;
464 Azidoblebbistatin, a photoreactive myosin inhibitor [44]. Our data suggest that
465 myosin 1f may be a novel pharmacological target for protecting photoreceptors
466 and preserving visual acuity.
467

468 ## Conclusions

469 In summary, our results show that myosin 1f plays a crucial role in microglia-
470 induced neuro-inflammation after retinal injury and photoreceptor degeneration
471 by regulating 2 classic pathways, MAPK and AKT, and thereby decreasing the
472 expression of inflammatory cytokines. Knockout of myosin 1f reduces the
473 intensity of the immune response and prevents cell death, suggesting that
474 myosin 1f can be inhibited to prevent a decline in visual acuity after
475 photoreceptor degeneration.
476

477 *Acknowledgements*

478 Not applicable.

Funding

This study was supported by the National Natural Science Foundation of China (81730026, 81771739) National Science and Technology Major Project (2017YFA0105301, 2019ZX09301113, SQ2018YFA090045-01),Science and Technology Commission of Shanghai Municipality (17411953000, 19495800700, 18JC1414100), the Program for Professor of Special Appointments (Eastern Scholar) at Shanghai Institutions of Higher Learning, the Top Young Talent Program of Shanghai, and the Innovative Research Team of High-level Local Universities in Shanghai.

Abbreviations

AD: Alzheimer's disease

HD: Huntington's disease

JNK: c-Jun NH2-terminal kinase

LPS: lipopolysaccharide

MAPK: mitogen-activated protein kinase

ONL: outer nuclear layer

PAMP: pathogen-associated molecular pattern

PCLP: pentachloropseudilin

PD: Parkinson's disease

PKB: protein kinase B

RPE: retinal pigment epithelium

RD: retinal detachment

RRD: rhegmatogenous retinal detachment

Availability of Data and Materials

The datasets analyzed during the current study are available from the corresponding author on reasonable request.

Ethics approval and consent to participate

All animal experiments were approved by the Ethics Committee of Jiao Tong University, Shanghai, China, and were conducted in compliance with the Association for Research in

Vision and Ophthalmology Statement for the Use of Animals in Ophthalmic and Vision Research.

Competing interests

The authors declare that they have no competing interests.

Consent for publication

Not applicable.

Authors' contributions

All authors read and approved the final manuscript.

Yimin Wang and Xiaohuan Zhao had full access to all of the data and take responsibility for the integrity of the data and the accuracy of the data analysis.

Concept and design: Yimin Wang, Xiaohuan Zhao, Feng Wang, Xiaodong Sun.

Acquisition, analysis, or interpretation of data: Yimin Wang, Xiaohuan Zhao, Min Gao, Yinong Guo, Yingying Qu, Yuhong Chen, Tong Li, Haiyun Liu.

Drafting of the manuscript: Yimin Wang.

Critical revision of the manuscript for important intellectual content: Xiaoling Wan, Mei Jiang, Feng Wang, Xiaodong Sun.

Statistical analysis: Yimin Wang, Xiaohuan Zhao

Obtained funding: Xiaodong Sun

Dr. Xiaodong Sun and Dr. Feng Wang are corresponding authors.

Authors' information

Yimin Wang, Xiaohuan Zhao, Min Gao, Xiaoling Wan, Yinong Guo, Yingying Qu, Yuhong Chen, Tong Li, Haiyun Liu, Mei Jiang, Feng Wang, Xiaodong Sun

Reference

1. Sene, A. and R.S. Apte, *Inflammation-Induced Photoreceptor Cell Death.* Advances in experimental medicine and biology, 2018. **1074**: p. 203-208.
2. Murakami, Y., et al., *Photoreceptor cell death and rescue in retinal detachment and degenerations.* Progress in Retinal and Eye Research, 2013. **37**: p. 114-140.
3. Vail, D., et al., *The Relative Impact of Patient, Physician, and Geographic Factors on Variation in Primary Rhegmatogenous Retinal Detachment Management.* Ophthalmology, 2020. **127**(1): p. 97-106.
4. Soni, C., D.P. Hainsworth, and A. Almony, *Surgical management of rhegmatogenous retinal detachment: a meta-analysis of randomized controlled trials.* Ophthalmology, 2013. **120**(7): p. 1440-1447.
5. Geiger, M., et al., *Predictors for recovery of macular function after surgery for primary macula-off rhegmatogenous retinal detachment.* International Ophthalmology, 2019. **40**(3): p. 609-616.
6. Wubben, T.J., C.G. Besirli, and D.N. Zacks, *Pharmacotherapies for Retinal Detachment.* Ophthalmology, 2016. **123**(7): p. 1553-1562.
7. Delyfer, M.-N., et al., *Transcriptomic analysis of human retinal detachment reveals both inflammatory response and photoreceptor death.* PloS one, 2011. **6**(12): p. e28791.
8. Yoshimura, T., et al., *Comprehensive analysis of inflammatory immune mediators in vitreoretinal diseases.* PloS one, 2009. **4**(12): p. e8158.
9. Nakazawa, T., et al., *Attenuated glial reactions and photoreceptor degeneration after retinal detachment in mice deficient in glial fibrillary acidic protein and vimentin.*

Investigative ophthalmology & visual science, 2007. **48**(6): p. 2760-2768.

10. Wang, M., et al., *Adaptive Müller cell responses to microglial activation mediate neuroprotection and coordinate inflammation in the retina.* Journal of neuroinflammation, 2011. **8**: p. 173.
11. Rutar, M., R. Natoli, and J.M. Provis, *Small interfering RNA-mediated suppression of Ccl2 in Müller cells attenuates microglial recruitment and photoreceptor death following retinal degeneration.* Journal of neuroinflammation, 2012. **9**: p. 221.
12. Rathnasamy, G., et al., *Retinal microglia - A key player in healthy and diseased retina.* Progress in neurobiology, 2019. **173**: p. 18-40.
13. Karlstetter, M., et al., *Retinal microglia: just bystander or target for therapy?* Progress in retinal and eye research, 2015. **45**: p. 30-57.
14. Vecino, E., et al., *Glia-neuron interactions in the mammalian retina.* Progress in retinal and eye research, 2016. **51**.
15. Lai, J.-L., et al., *Indirubin Inhibits LPS-Induced Inflammation via TLR4 Abrogation Mediated by the NF-kB and MAPK Signaling Pathways.* Inflammation, 2017. **40**(1).
16. Manning, B.D. and A. Toker, *AKT/PKB Signaling: Navigating the Network.* Cell, 2017. **169**(3): p. 381-405.
17. Nüchel, J., et al., *TGFB1 is secreted through an unconventional pathway dependent on the autophagic machinery and cytoskeletal regulators.* Autophagy, 2018. **14**(3): p. 465-486.
18. Piedra-Quintero, Z.L., et al., *Myosin 1F Regulates M1-Polarization by Stimulating Intercellular Adhesion in Macrophages.* Frontiers in Immunology, 2019. **9**.
19. Vandenboom, R., *Modulation of Skeletal Muscle Contraction by Myosin Phosphorylation.* Compr Physiol, 2016. **7**(1): p. 171-212.
20. Titus, M.A., *Myosin-Driven Intracellular Transport.* Cold Spring Harb Perspect Biol, 2018. **10**(3).

602 21. Jung, G., X. Wu, and J.A. Hammer, 3rd, *Dictyostelium mutants*
603 *lacking multiple classic myosin I isoforms reveal combinations*
604 *of shared and distinct functions.* J Cell Biol, 1996. **133**(2): p.
605 305-23.
606 22. Jung, G. and J.A. Hammer, 3rd, *Generation and characterization*
607 *of Dictyostelium cells deficient in a myosin I heavy chain*
608 *isoform.* J Cell Biol, 1990. **110**(6): p. 1955-64.
609 23. Wessels, D., et al., *Myosin IB null mutants of Dictyostelium*
610 *exhibit abnormalities in motility.* Cell Motil Cytoskeleton,
611 1991. **20**(4): p. 301-15.
612 24. Temesvari, L.A., et al., *Examination of the endosomal and*
613 *lysosomal pathways in Dictyostelium discoideum myosin I*
614 *mutants.* J Cell Sci, 1996. **109 (Pt 3)**: p. 663-73.
615 25. Guo, Y., et al., *An improved method for establishment of murine*
616 *retinal detachment model and its 3D vascular evaluation.*
617 Experimental eye research, 2020. **193**: p. 107949.
618 26. Gao, M., et al., *xCT regulates redox homeostasis and promotes*
619 *photoreceptor survival after retinal detachment.* Free Radic
620 Biol Med, 2020. **158**: p. 32-43.
621 27. Henn, A., et al., *The suitability of BV2 cells as alternative*
622 *model system for primary microglia cultures or for animal*
623 *experiments examining brain inflammation.* ALTEX, 2009. **26**(2):
624 p. 83-94.
625 28. Zhou, T., et al., *Microglia Polarization with M1/M2 Phenotype*
626 *Changes in rd1 Mouse Model of Retinal Degeneration.* Frontiers
627 in neuroanatomy, 2017. **11**: p. 77.
628 29. Krigel, A., et al., *Light-induced retinal damage using*
629 *different light sources, protocols and rat strains reveals LED*
630 *phototoxicity.* Neuroscience, 2016. **339**: p. 296-307.
631 30. Tisi, A., et al., *Up-regulation of pro-angiogenic pathways and*
632 *induction of neovascularization by an acute retinal light*
633 *damage.* Sci Rep, 2020. **10**(1): p. 6376.
634 31. Salvermoser, M., et al., *Myosin 1f is specifically required for*

neutrophil migration in 3D environments during acute inflammation. Blood, 2018. **131**(17): p. 1887-1898.

32. Wang, Y., et al., *Myosin1f-mediated neutrophil migration contributes to acute neuroinflammation and brain injury after stroke in mice.* Journal of neuroinflammation, 2019. **16**(1): p. 77.

33. Tang, Y. and W. Le, *Differential Roles of M1 and M2 Microglia in Neurodegenerative Diseases.* Mol Neurobiol, 2016. **53**(2): p. 1181-1194.

34. Hendrickx, D.A.E., et al., *Staining of HLA-DR, Iba1 and CD68 in human microglia reveals partially overlapping expression depending on cellular morphology and pathology.* J Neuroimmunol, 2017. **309**: p. 12-22.

35. Walker, D.G. and L.F. Lue, *Immune phenotypes of microglia in human neurodegenerative disease: challenges to detecting microglial polarization in human brains.* Alzheimers Res Ther, 2015. **7**(1): p. 56.

36. Sosna, J., et al., *Early long-term administration of the CSF1R inhibitor PLX3397 ablates microglia and reduces accumulation of intraneuronal amyloid, neuritic plaque deposition and pre-fibrillar oligomers in 5XFAD mouse model of Alzheimer's disease.* Mol Neurodegener, 2018. **13**(1): p. 11.

37. Tahmasebi, F., et al., *Effect of the CSF1R inhibitor PLX3397 on remyelination of corpus callosum in a cuprizone-induced demyelination mouse model.* J Cell Biochem, 2019. **120**(6): p. 10576-10586.

38. Merry, T.L., et al., *The CSF1 receptor inhibitor pexidartinib (PLX3397) reduces tissue macrophage levels without affecting glucose homeostasis in mice.* Int J Obes (Lond), 2020. **44**(1): p. 245-253.

39. Stansley, B., J. Post, and K. Hensley, *A comparative review of cell culture systems for the study of microglial biology in Alzheimer's disease.* J Neuroinflammation, 2012. **9**: p. 115.

40. Pardue, M.T. and R.S. Allen, *Neuroprotective strategies for retinal disease.* Progress in retinal and eye research, 2018. **65**: p. 50-76.
41. Daruich, A., et al., *Iron is neurotoxic in retinal detachment and transferrin confers neuroprotection.* Science advances, 2019. **5**(1): p. eaau9940.
42. Chung, C.L., et al., *Roles of Myosin-Mediated Membrane Trafficking in TGF-β Signaling.* Int J Mol Sci, 2019. **20**(16).
43. McConnell, R.E. and M.J. Tyska, *Leveraging the membrane - cytoskeleton interface with myosin-1.* Trends in cell biology, 2010. **20**(7): p. 418-426.
44. Heissler, S.M. and J.R. Sellers, *Various Themes of Myosin Regulation.* Journal of molecular biology, 2016. **428**(9 Pt B): p. 1927-1946.
45. Piedra-Quintero, Z.L., et al., *Myosin 1F Regulates M1-Polarization by Stimulating Intercellular Adhesion in Macrophages.* Frontiers in immunology, 2018. **9**: p. 3118.
46. A, L., et al., *Rescue of Retinal Degeneration in rd1 Mice by Intravitreally Injected Metformin.* Frontiers in molecular neuroscience, 2019. **12**: p. 102.
47. Mukherjee, S., et al., *A Microglial Signature Directing Human Aging and Neurodegeneration-Related Gene Networks.* Front Neurosci, 2019. **13**: p. 2.
48. Silverman, S.M. and W.T. Wong, *Microglia in the Retina: Roles in Development, Maturity, and Disease.* Annual review of vision science, 2018. **4**: p. 45-77.
49. Du, L., et al., *Role of Microglia in Neurological Disorders and Their Potentials as a Therapeutic Target.* Molecular neurobiology, 2017. **54**(10): p. 7567-7584.
50. Block, M.L., L. Zecca, and J.-S. Hong, *Microglia-mediated neurotoxicity: uncovering the molecular mechanisms.* Nature reviews. Neuroscience, 2007. **8**(1): p. 57-69.
51. Colonna, M. and O. Butovsky, *Microglia Function in the Central*

Nervous System During Health and Neurodegeneration. Annual review of immunology, 2017. **35**: p. 441-468.

52. Okunuki, Y., et al., *Microglia inhibit photoreceptor cell death and regulate immune cell infiltration in response to retinal detachment.* Proceedings of the National Academy of Sciences of the United States of America, 2018. **115**(27): p. E6264-E6273.

53. Sun, Y., et al., *Signaling pathway of MAPK/ERK in cell proliferation, differentiation, migration, senescence and apoptosis.* Journal of receptor and signal transduction research, 2015. **35**(6): p. 600-604.

54. Kyriakis, J.M. and J. Avruch, *Mammalian MAPK signal transduction pathways activated by stress and inflammation: a 10-year update.* Physiological reviews, 2012. **92**(2): p. 689-737.

55. Santa-Cecília, F.V., et al., *Doxycycline Suppresses Microglial Activation by Inhibiting the p38 MAPK and NF-kB Signaling Pathways.* Neurotoxicity research, 2016. **29**(4): p. 447-459.

56. Feng, N., Y. Jia, and X. Huang, *Exosomes from adipose-derived stem cells alleviate neural injury caused by microglia activation via suppressing NF-kB and MAPK pathway.* Journal of neuroimmunology, 2019. **334**: p. 576996.

57. Nam, H.Y., et al., *Ibrutinib suppresses LPS-induced neuroinflammatory responses in BV2 microglial cells and wild-type mice.* J Neuroinflammation, 2018. **15**(1): p. 271.

58. Zhang, Y., et al., *Kinase AKT controls innate immune cell development and function.* Immunology, 2013. **140**(2): p. 143-52.

59. Qin, S., et al., *Sulforaphane attenuates microglia-mediated neuronal necroptosis through down-regulation of MAPK/NF-κB signaling pathways in LPS-activated BV-2 microglia.* Pharmacological research, 2018. **133**: p. 218-235.

60. Frakes, A.E., et al., *Microglia induce motor neuron death via the classical NF-κB pathway in amyotrophic lateral sclerosis.* Neuron, 2014. **81**(5): p. 1009-1023.

61. Rafiq, N.B.M., et al., *A mechano-signalling network linking*

microtubules, myosin IIA filaments and integrin-based adhesions. Nature Materials, 2019. **18**(6): p. 638-649.

62. Choi, C., et al., *Integrin β1, myosin light chain kinase and myosin IIA are required for activation of PI3K-AKT signaling following MEK inhibition in metastatic triple negative breast cancer.* Oncotarget, 2016. **7**(39): p. 63466-63487.

63. Chinthalapudi, K., et al., *Mechanism and specificity of pentachloropseudilin-mediated inhibition of myosin motor activity.* J Biol Chem, 2011. **286**(34): p. 29700-8.

64. Heissler, S.M. and J.R. Sellers, *Various Themes of Myosin Regulation.* J Mol Biol, 2016. **428**(9 Pt B): p. 1927-46.

65. Rauscher, A., et al., *Targeting Myosin by Blebbistatin Derivatives: Optimization and Pharmacological Potential.* Trends Biochem Sci, 2018. **43**(9): p. 700-713.

Figure legends

Figure 1

Transcriptome analysis of human retinal detachment. A. Identification of differential expressed genes (DRGs) were set as |FC|>1.5 and p<0.05. Red dots on the volcano plot (A) represent up-regulated genes while blue dots represent down-regulated genes. B-C. Gene ontology analysis. Cellular components analysis (B) and biological process analysis (C) showed possible functions of DEGs. D. Gene-set enrichment analysis (GSEA) also revealed possible pathways possibly correlated to RD, including inflammatory response. E-F. Expression pattern of myosins. Heatmap (E) demonstrated the most evaluated myosin, myosin 1f, with a FC=1.786 (F). G. The fold changes of at different RD duration.

Figure 2

Myosin 1f is up-regulated after mouse model of retinal detachment. A. The expression of myosin 1f at day 1, day 3, day 7, it reached to peak at day 3 (A).

The expression value is calculated by the optical density ration of myosin 1f and GAPDH. B. Representative image of eye sections stained for F4/80 (green), myosin 1f (red) and dapi (blue). The eyeballs were taken down at day 3 after RD. C. Representative image of eye sections stained for IBA1 (green), myosin 1f (red) and dapi (blue) (day 3). D. Eye sections stained for GFAP (green), myosin 1f (red) and dapi (blue) (day 3). E-F. Myosin 1f is also up-regulated in rd1 mouse(E) (day 7 after birth) and light-injured retina(F) (day 5). G. Retinal sections of rd1 mice (day 7 after birth) stained for F4/80 (green), myosin 1f (red) and dapi (blue). H. Retinal sections of light-injured retina (day 5) stained for F4/80 (green), myosin 1f (red) and dapi (blue).

Figure 3

Observation of myosin 1f -/- mice after retinal detachment model. A. Two groups of mice, myosin 1f-/- and WT, were sacrificed at day 3. B-C. HE staining showed the thickness of ONL on detached retina (day 3) of two groups (B). Scale bar, 100μm. Measurements of ONL were taken by image J (C), and data

were presented as mean±SEM, unpaired t test, *P < 0.05, **P < 0.01, ***P < 0.001, ****P < 0.0001. D-E. Representative tunel staining in ONL (in green) (3 days after induction of RD) showed apoptosis of photoreceptors, scale bar, 100μm(D), quantification of tunel positive cells in ONL (E) revealed the significance, data were presented as mean±SEM, unpaired t test, *P < 0.05, **P < 0.01, ***P < 0.001, ****P < 0.0001.

Figure 4

Knock out of myosin 1f affects the function of microglia. A. Flatmount of detached retina of WT and myosin 1f -/- mice, stained by IBA1 (in red), showed morphology of microglia. Scale bar, 25μm. B-C. Skeleton analysis (B) and sholl analysis (C) were conducted to quantify microglia morphology. The less average branch length is, the more activated microglia is; Similarly, the less interaction number is, the more activated microglia is. D-E. ELISA analysis of IL-1β (D) and TNF-α (E) in detached retina of WT and myo1f KO mice (day 3). F-G. Qpcr analysis of IL-1β and TNF-α in detached retina at day 3 (F) and

CD68 (G) at day 1. Data were presented as mean±SEM, unpaired t test, *P < 0.05, **P < 0.01, ***P < 0.001, ****P < 0.0001.

Figure 5

Elimination of microglia reverse the protective effect of myosin 1f deficiency. A. PLX3397 was given to WT and myosin 1f-/- mice everyday from day 1 to day 6, the mice were sacrificed at day 7, 3 days after mouse model of retinal detachment (day 4). B. Representative HE staining showed the thickness of ONL on detached retina (scale bar, 50μm), representative tunel staining in ONL (in green) (3 days after induction of RD) (scale bar, 100μm) showed apoptosis of photoreceptors after microglia elimination. C. Quantification of ONL thickness and tunel positive cells in ONL between two groups. D-E. Qpcr analysis demonstrated the fold change of IL-1β, TNF-α and CD68 (day 3), data were presented as mean±SEM, unpaired t test, *P < 0.05, **P < 0.01, ***P < 0.001, ****P < 0.0001.

Figure 6

Myosin 1f affects the activation of microglia by regulating NF-κb and MAPK pathways. A. In vitro, western blot showed that myosin 1f is up-regulated after stimulated by LPS (100ng/ml) for 24 hours, the expression value is calculated by the optical density ration of myosin 1f and GAPDH. B. The expression of IL-1β (qpcr) and TNF-α (ELISA) at every time point. C-D. After siRNA on BV2 cell lines, we detected the expression of myosin 1f by western blot (C). Three sequences of siRNA (768,1413,2772) were designed to knock down myosin 1f, 2662 were chosen to further confirm the efficiency (D). E. ELISA analysis of IL-1β and TNF-α after knock down myosin 1f. F. In vitro, wb analysis showed expression pattern of NF-κb and MAPK pathways. All the quantification of phosphorylation protein is calculated by the optical density ration of phosphorylation protein and its corresponding protein. G. All the quantification of phosphorylation protein is calculated by the optical density ration of phosphorylation protein and GAPDH. Data were presented as mean±SEM, unpaired t test, *P < 0.05, **P < 0.01, ***P < 0.001, ****P < 0.0001.

Supplementary figure 1

A. Gene-set enrichment analysis (GSEA) also revealed possible pathways possibly correlated to RD, including interferon-gamma response, IL-6-STAT3 signaling, complement, IL-2-STAT5 signaling.

Supplementary figure 2

Myosin 1f deficiency does not affect the structure and function of retina. A-D. OCT (A, B) and HE (C, D) staining reflects the thickness of WT and myosin 1f-/- mouse retina. Data were presented as mean±SEM, unpaired t test, n.c. $P > 0.05$. E. Electroretinogram of WT and myosin 1f mice, more than 20 weeks- year-old.

Data were presented as mean±SEM, unpaired t test, $^{*}P < 0.05$, $^{**}P < 0.01$, $^{***}P < 0.001$, $^{****}P < 0.0001$.

Supplementary figure 3

A-B. Fundus photography (A) and HE (B) showed detachment of RPE and photoreceptor (day 3). C. IBA1+ cell counts of the stretched preparation of retina after retinal detachment. D The cell count of both F4/80+ and IBA1+ cells infiltrated into outer nuclear layer. Data were presented as mean±SEM, unpaired t test, *P < 0.05, **P < 0.01, ***P < 0.001, ****P < 0.0001.

Figures

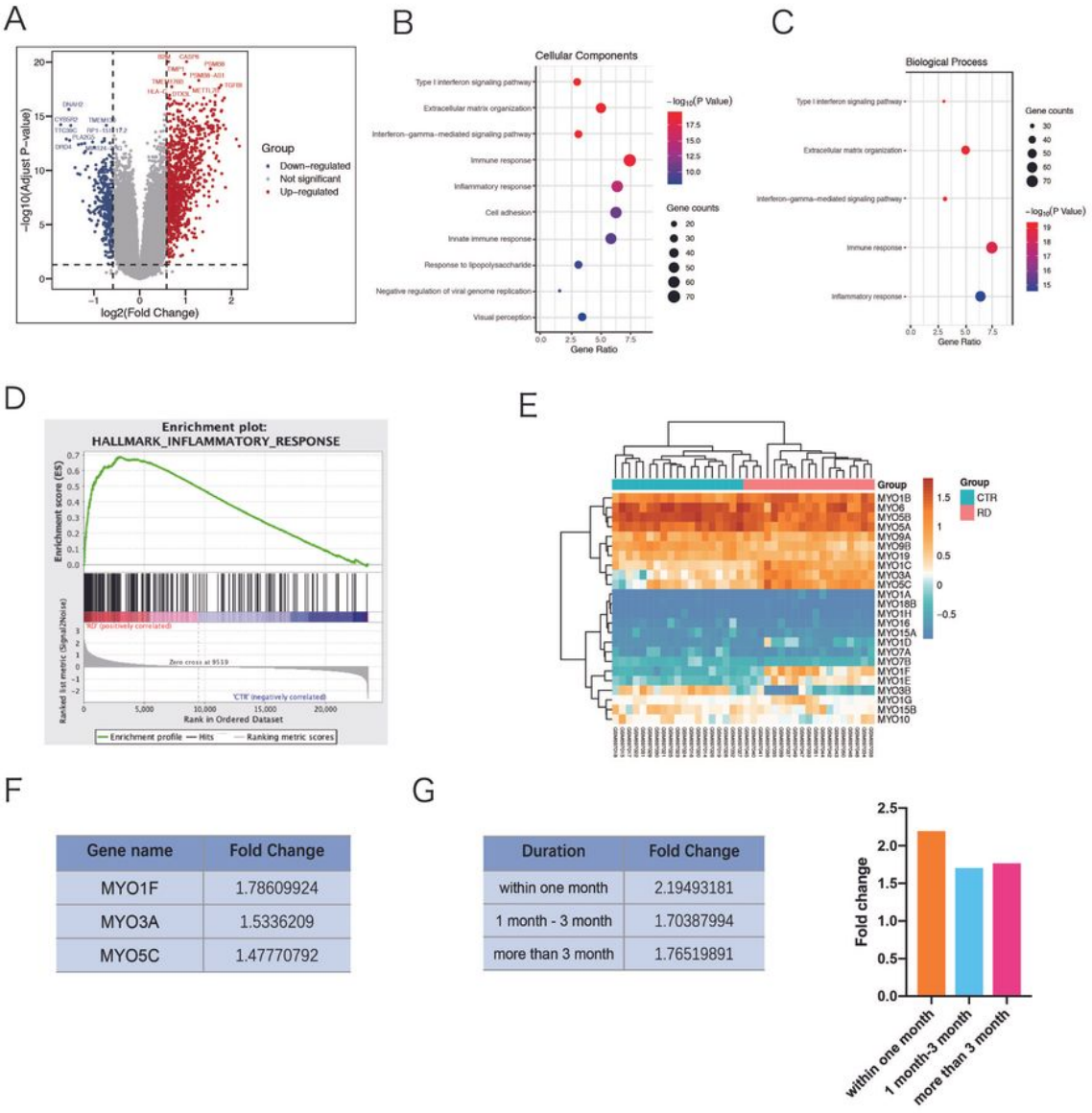

Gene name	Fold Change
MYO1F	1.78609924
MYO3A	1.5336209
MYO5C	1.47770792

Duration	Fold Change
within one month	2.19493181
1 month - 3 month	1.70387994
more than 3 month	1.76519891

Figure 1

Transcriptome analysis of human retinal detachment. A. Identification of differential expressed genes (DRGs) were set as |FC|>1.5 and p<0.05. Red dots on the volcano plot (A) represent up-regulated genes while blue dots represent down-regulated genes. B-C. Gene ontology analysis. Cellular components

analysis (B) and biological process analysis (C) showed possible functions of DEGs. D. Gene-set enrichment analysis (GSEA) also revealed possible pathways possibly correlated to RD, including inflammatory response. E-F. Expression pattern of myosins. Heatmap (E) demonstrated the most evaluated myosin, myosin 1f, with a FC=1.786 (F). G. The fold changes of at different RD duration.

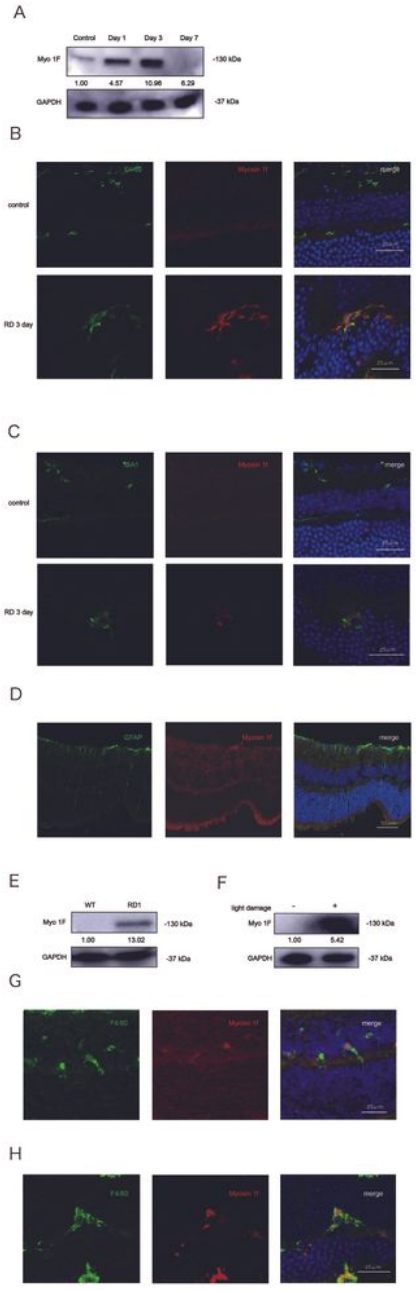

Figure 2

Myosin 1f is up-regulated after mouse model of retinal detachment. A. The expression of myosin 1f at day 1, day 3, day 7, it reached to peak at day 3 (A). The expression value is calculated by the optical density ration of myosin 1f and GAPDH. B. Representative image of eye sections stained for F4/80 (green), myosin 1f (red) and dapi (blue). The eyeballs were taken down at day 3 after RD. C. Representative image of eye sections stained for IBA1 (green), myosin 1f (red) and dapi (blue) (day 3). D. Eye sections stained for GFAP (green), myosin 1f (red) and dapi (blue) (day 3). E-F. Myosin 1f is also up-regulated in rd1 mouse(E) (day 7 after birth) and light-injured retina(F) (day 5). G. Retinal sections of rd1 mice (day 7 after birth) stained for F4/80 (green), myosin 1f (red) and dapi (blue). H. Retinal sections of light-injured retina (day 5) stained for F4/80 (green), myosin 1f (red) and dapi (blue).

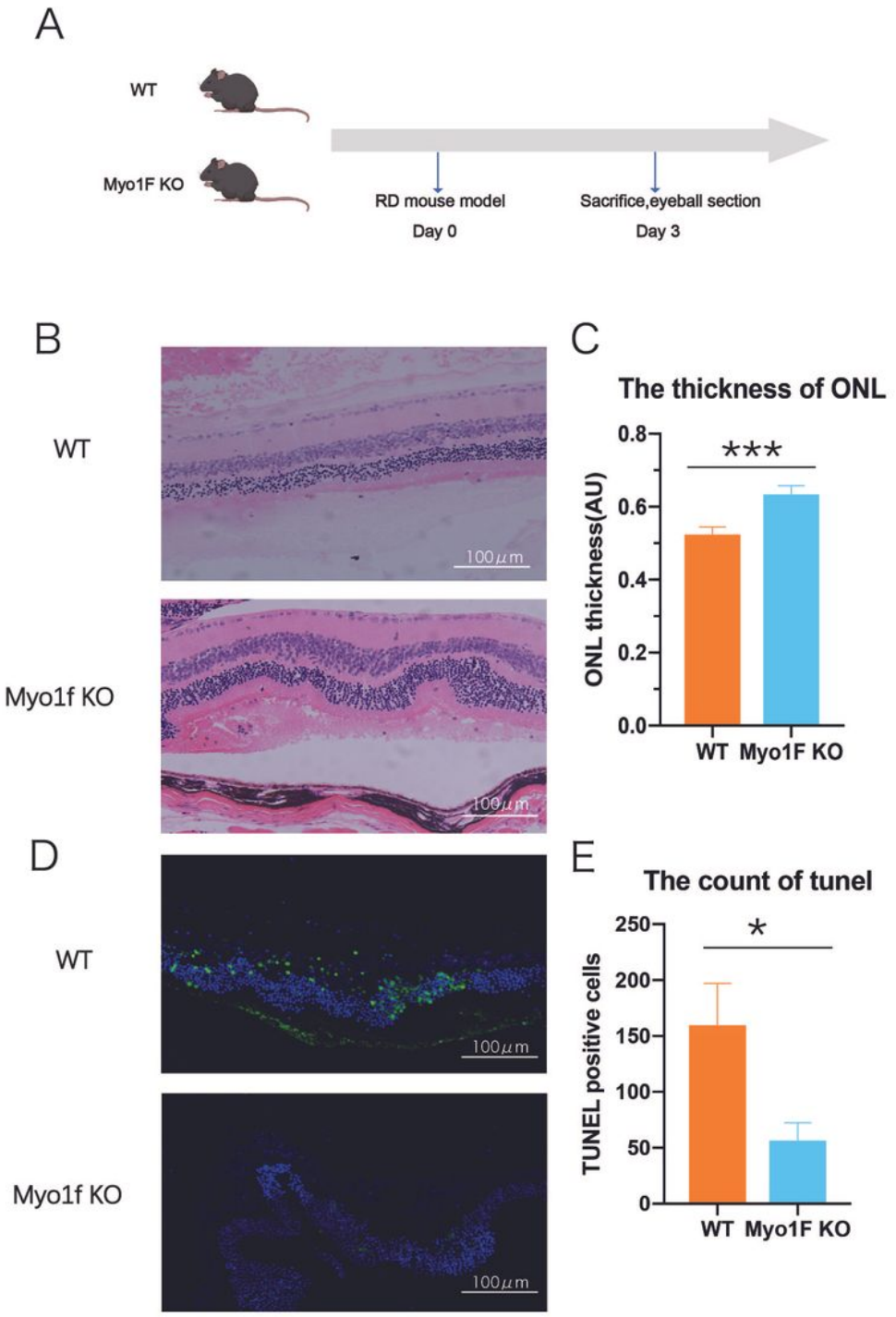

Figure 3

Observation of myosin 1f -/- mice after retinal detachment model. A. Two groups of mice, myosin 1f-/- and WT, were sacrificed at day 3. B-C. HE staining showed the thickness of ONL on detached retina (day 3) of two groups (B). Scale bar, 100μm. Measurements of ONL were taken by image J (C), and data were presented as mean±SEM, unpaired t test, *P < 0.05, **P < 0.01, ***P < 0.001, ****P < 0.0001. D-E. Representative tunel staining in ONL (in green) (3 days after induction of RD) showed apoptosis of

photoreceptors, scale bar, 100μm(D), quantification of tunel positive cells in ONL (E) revealed the significance, data were presented as mean±SEM, unpaired t test, *P < 0.05, **P < 0.01, ***P < 0.001, ****P < 0.0001.

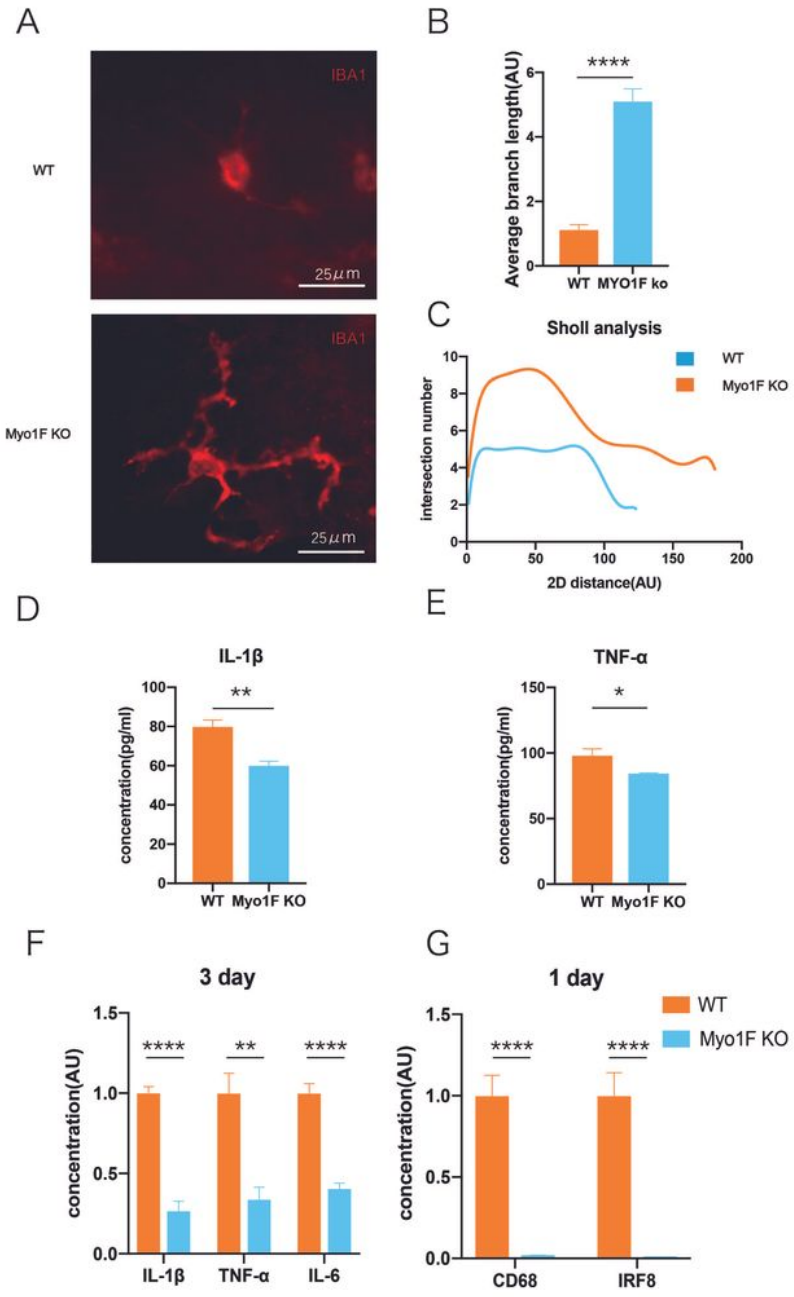

Figure 4

Knock out of myosin 1f affects the function of microglia. A. Flatmount of detached retina of WT and myosin 1f -/- mice, stained by IBA1 (in red), showed morphology of microglia. Scale bar, 25μm. B-C.

Skeleton analysis (B) and sholl analysis (C) were conducted to quantify microglia morphology. The less average branch length is, the more activated microglia is; Similarly, the less interaction number is, the more activated microglia is. D-E. ELISA analysis of IL-1β (D) and TNF-α (E) in detached retina of WT and myo1f KO mice (day 3). F-G. Qpcr analysis of IL-1β and TNF-α in detached retina at day 3 (F) and CD68 (G) at day 1. Data were presented as mean±SEM, unpaired t test, *P < 0.05, **P < 0.01, ***P < 0.001, ****P < 0.0001.

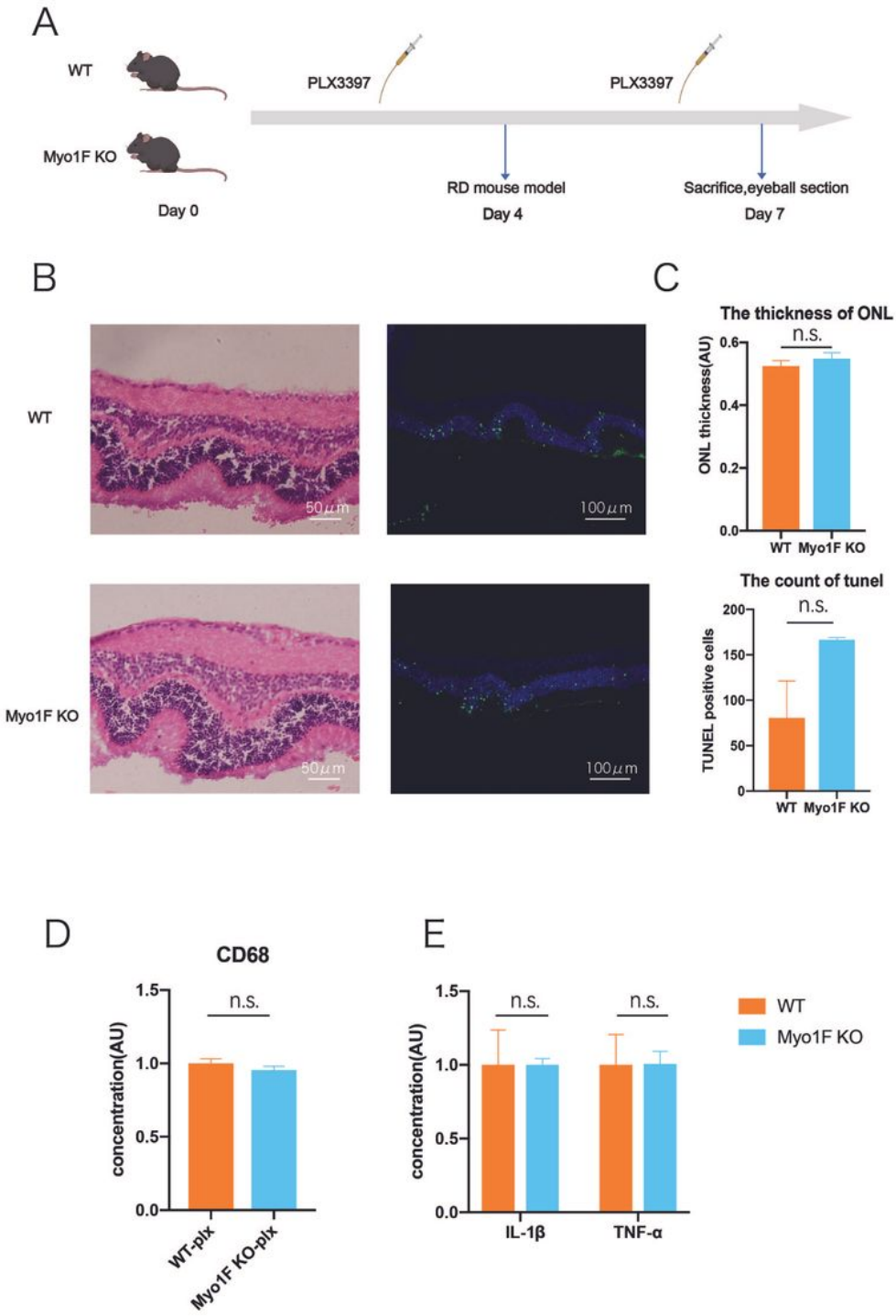

Figure 5

Elimination of microglia reverse the protective effect of myosin 1f deficiency. A. PLX3397 was given to WT and myosin 1f-/- mice everyday from day 1 to day 6, the mice were sacrificed at day 7, 3 days after mouse model of retinal detachment (day 4). B. Representative HE staining showed the thickness of ONL on detached retina (scale bar, 50μm), representative tunel staining in ONL (in green) (3 days after induction of RD) (scale bar, 100μm) showed apoptosis of photoreceptors after microglia elimination. C. Quantification of ONL thickness and tunel positive cells in ONL between two groups. D-E. Qpcr analysis demonstrated the fold change of IL-1β, TNF-α and CD68 (day 3), data were presented as mean±SEM, unpaired t test, *P < 0.05, **P < 0.01, ***P < 0.001, ****P < 0.0001.

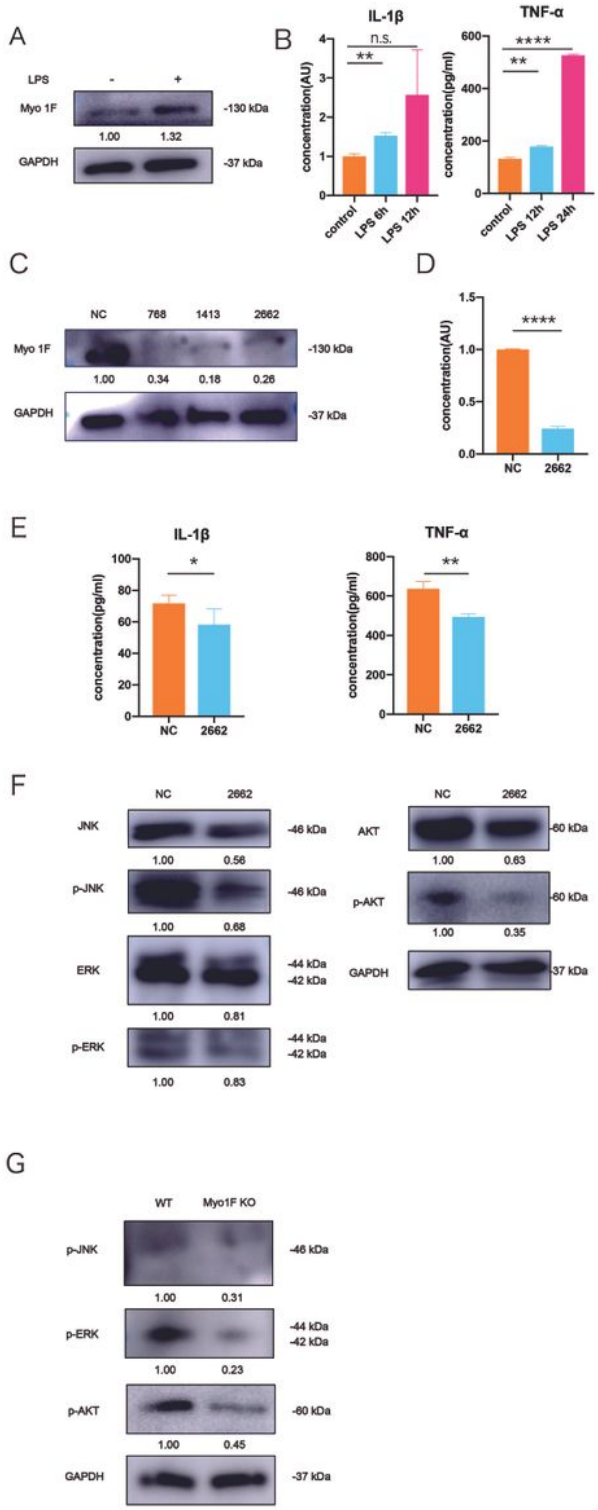

Figure 6

Myosin 1f affects the activation of microglia by regulating NF-κb and MAPK pathways. A. In vitro, western blot showed that myosin 1f is up-regulated after stimulated by LPS (100ng/ml) for 24 hours, the expression value is calculated by the optical density ration of myosin 1f and GAPDH. B. The expression of IL-1β (qpcr) and TNF-α (ELISA) at every time point. C-D. After siRNA on BV2 cell lines, we detected the expression of myosin 1f by western blot (C). Three sequences of siRNA (768,1413,2772) were designed to

knock down myosin 1f, 2662 were chosen to further confirm the efficiency (D). E. ELISA analysis of IL-1β and TNF-α after knock down myosin 1f. F. In vitro, wb analysis showed expression pattern of NF-κb and MAPK pathways. All the quantification of phosphorylation protein is calculated by the optical density ration of phosphorylation protein and its corresponding protein. G. All the quantification of phosphorylation protein is calculated by the optical density ration of phosphorylation protein and GAPDH. Data were presented as mean±SEM, unpaired t test, *P < 0.05, **P < 0.01, ***P < 0.001, ****P < 0.0001.

Supplementary Files

This is a list of supplementary files associated with this preprint. Click to download.

- supplementary1.jpg
- supplementary2.jpg
- supplementary3.jpg